Accepted Manuscript

On the Curie temperature and Nishizawa horn in the Al-Co-Ni system

Yang Zhou, Philip Nash

PII: S0925-8388(18)34224-5

DOI: https://doi.org/10.1016/j.jallcom.2018.11.103

Reference: JALCOM 48329

To appear in: *Journal of Alloys and Compounds*

Received Date: 3 May 2018

Revised Date: 15 October 2018

Accepted Date: 8 November 2018

Please cite this article as: Y. Zhou, P. Nash, On the Curie temperature and Nishizawa horn in the Al-Co-Ni system, *Journal of Alloys and Compounds* (2018), doi: https://doi.org/10.1016/j.jallcom.2018.11.103.

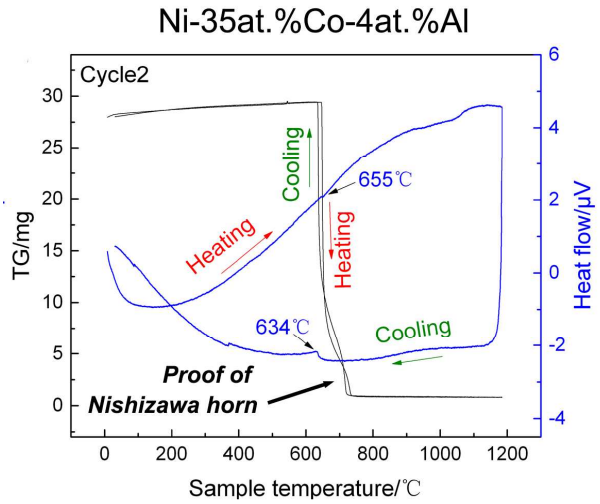

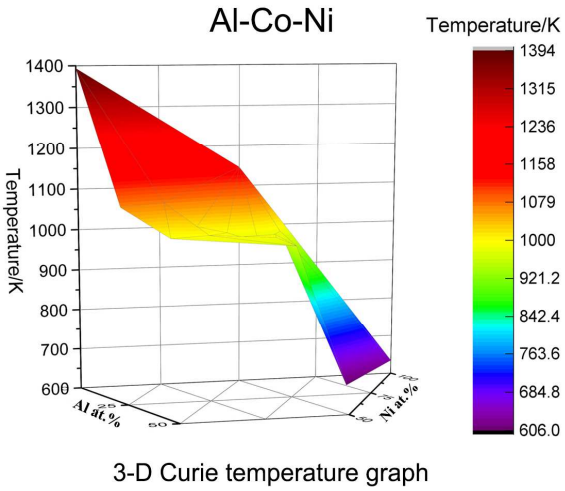

3-D Curie temperature graph

On the Curie temperature and Nishizawa Horn in the Al-Co-Ni system

Yang Zhou[1,2], Philip Nash[1]

ORCID: Yang Zhou: 0000-0002-5543-9366, Philip Nash: 0000-0003-2975-8512

1. Thermal Processing Technology Center, Illinois Institute of Technology, Chicago, IL 60616, USA

2. Shanghai Key Laboratory of Advanced High-temperature Materials and Precision Forming, Shanghai Jiao Tong University, No. 800, Dongchuan Road, Shanghai, 200240, China

Abstract

There have been extensive reports on the phase diagram and magnetic properties of the Al-Co-Ni system. However, a systematic investigation of the Curie temperatures in this alloy system is still lacking. In this work, the Curie temperature in the fcc phase field of the Al-Co-Ni alloy system was studied using a simultaneous magnetic balance and differential scanning calorimeter method. The Curie temperature contour map was constructed according to the measured results and an Exponential2D fitting function using Originlab® was obtained, which provides a useful tool for estimating the Curie temperature in Al-Co-Ni alloys. The experimental technique provides a novel method of detecting phase transformations and precipitation based on analyzing the heat effects and magnetic behavior of the alloys in the presence or absence of a magnetic field. Experimental results from this technique provide the first evidence for the occurrence of a Nishizawa horn in this system as predicted using Thermo-Calc®.

[1] Corresponding author: Yang Zhou, email yzhou76@sjtu.edu.cn.

Keywords: Magnetic measurements; high-temperature alloys; precipitation; thermal analysis.

1. Introduction

There is intense interest in the Al-Co-Ni alloy system due to their functional and structural properties, with potential applications such as ferromagnetic shape memory alloys (FSMA)[1–6], high-temperature structural alloys and catalysts[7,8]. Several studies have been reported on the phase transformations, microstructural evolution and magnetic properties in this system[3,4,9,10]. Phase equilibria were established by various researchers, including isothermal sections and liquidus projection both experimentally and computationally[7,11–15]. The wide applicability of Al-Co-Ni alloys depends on the specific alloy composition and phases present, for instance, the β phase ((Ni,Co)Al: B2) that undergoes a thermoelastic martensitic transformation from B2 to $L1_0$ accounts for the shape memory effect, which makes Al-Co-Ni alloys promising as shape memory alloys (SMA)[12,13,16]; the precipitation of γ' from the γ matrix is the basis for high-temperature structural alloys[7], where γ is the Ni solid solution FCC austenite phase and γ' is an intermetallic phase based on Ni_3Al which has an ordered FCC $L1_2$ structure. It is therefore fundamentally important for alloy design to have a good understanding of the microstructure, phase transformation and precipitation behavior in this system. Fig. 1 shows the calculated isothermal section of the Al-Co-Ni system at 800°C using Thermo-Calc® with the TCNI8 database. BCC_B2 represents the disordered β phase; BCC_B2#2 represents the ordered β phase; FCC_L12 is the ferromagnetic γ phase (γ_f), FCC_L12#2 is the ordered γ' (Ni_3Al) phase and FCC_L12#3, is the paramagnetic γ phase

(γ_p). In the Al-poor area, there are three main phases γ, γ' and β. It can be seen that Thermo-Calc® predicts the occurrence of a Nishizawa horn which is an extension from the binary Co-Al system. This results in a phase separation of the γ phase into ferromagnetic and paramagnetic components. It should be noted that the isothermal section in Fig. 1 corresponds to a temperature close to the four phase invariant reaction involving the two γ phases, γ' and β phase[9]. This is the reason that the three-phase field $\gamma_p+\gamma_f+\gamma'$ is very narrow.

The Curie temperature (Tc) is essential information for magnetic alloys, and is defined as the critical temperature where the material loses its ferromagnetic property. Since it is a second order transition, the Curie transition can be difficult to observe from a DSC curve. On the other hand it is easy to measure Tc with a vibrating sample magnetometer (VSM)[4] or through a thermomagnetic analysis (TMA) method[17]. But for binary or ternary alloy systems, it becomes complicated due to the existence of multiple phases and composition variations with temperature. Thermogravimetry (TG) where the mass of the sample is measured vs. temperature provides no information of a sample that neither loses nor gains mass during the experiment. However, in the presence of a constant applied magnetic field TG becomes a very sensitive indicator of ferromagnetic phenomena, due to the magnetic force present in addition to gravitational force. Thus, from the mass vs. temperature curve, phase transformation and precipitation process can be observed and analyzed if a ferromagnetic phase is involved. Several recently published papers discussed the martensitic transformation in Al-Co-Ni and measured T_C in a limited composition range[4,18–20]. However, a systematic study of the Curie temperature in the Al-Co-Ni system is still lacking. In this paper, we have measured the Curie point of Al-Co-Ni samples

in the Al-poor region and provided analysis of the thermogravimetric curves in the presence of a magnetic field to provide insight into monitoring phase transformations including the Nishizawa horn and precipitation phenomena.

2. Experimental Procedures

In this study, a total of 19 alloys were prepared by arc melting elemental materials of Al shot (99.99% purity), Ni shot (99.99% purity) and Co pieces (99.99% purity). The nominal compositions of the Al-Co-Ni alloy samples used for the TG-DSC analysis and the measured mass, under gravitational field only, are listed in Table 1. The alloy compositions are in the range of (5-75) at.%Ni, (10-70) at.%Co, and (4-30) at.%Al, and are identified by their respective atomic % compositions as shown in Table 1, henceforth referred to as Ni X-Y (X denotes the atomic percent of Co and Y is the atomic percent of Al). All samples were homogenized at 1200°C for 24h after arc-melting in order to transform the as-cast structure and reduce chemical inhomogeneity. Subsequently, alloys No.1-14 were cold rolled to reduce the grain size and further remove chemical segregation. The remaining alloys were too brittle to be cold rolled. All samples were annealed at 1100°C or 1200°C for 24h to 94h under Ar protection, followed by quenching in water. In order to investigate the microstructural evolution, lower temperature annealing was also performed at 800°C(168h), 600°C(336h) and 550°C(336h).

The thermo-magnetic analysis was performed on a modified Setaram TG/DSC SETSYS instrument with an external electromagnetic field applied[21]. In this way, it is easy to control the magnetic field by adjusting the current of the power supply and thereby measure the Curie temperature of the alloys. After placing the sample in the TG balance the

balance was zeroed before turning on the magnetic field. When the magnetic field is applied there is a downward force imposed on the sample, which manifests as a mass change on the balance. The device is not a traditional Guoy or Faraday balance. Here we are not trying to determine accurate magnetic susceptibility data, only aiming to observe relative changes in the magnetic moment within a sample which are manifested as an apparent change in mass. The Setaram TGA is an electronically balanced system so the position of the sample in the magnetic field does not change during any change in magnetic susceptibility. The heating and cooling rate for all experiments was 5°C/min. Optical microscopy, X-ray Diffraction (XRD) and Scanning Electron Microscopy (SEM) were used to characterize the microstructure and phase changes at different aging temperatures. Thermo-Calc® with the TCNI8 database was used to calculate an isothermal section of the alloy system corresponding to 800°C. OriginPro 9.2 was used to construct the Curie temperature contour map and to obtain the fitting functions.

3.Results

Seven typical TG-DSC results are discussed below according to the Al content (at.%) for alloys ranging from 4 at.% Al to 30 at.% Al. Two thermal cycles were performed on each sample to confirm reproducibility. The TG-DSC curves for all other alloys are included in a supplementary data file (Fig. S6-S16).

3.1 4 at.%Al

Fig. 2 shows the TG and DSC heat flow curves vs. temperature of the Ni 35-4 sample in two thermal cycles. An obvious Curie transformation occurs during the heating and

cooling cycles. Note that the effects that can give rise to an apparent mass change are caused by three factors: the magnetic susceptibility of a phase; the amount of ferromagnetic phase; phase composition, where the amount of ferromagnetic phase refers to the volume fraction of γ_f phase in this work, while phase composition refers to the concentration of Co, Ni and Al in a phase. In Fig. 2a), during the first cycle, it can be seen from the TG curve that at low temperature the sample remains ferromagnetic with the apparent sample mass remaining almost constant at 26mg until 650°C when the effective mass drops sharply to zero, due to the Curie transformation from the ferromagnetic to paramagnetic sample state.

On cooling from 1200°C, the reverse transformation from paramagnetic to ferromagnetic state was observed. However, there is a difference between the first cycle heating and cooling process. On cooling, the TG curve increases slowly from zero, beginning at 760°C, followed by a rapid increase from around 630°C. A possible explanation is that according to the phase diagram of the Al-Co-Ni system, during cooling from 760°C, a second phase, γ', precipitated from the matrix, changing the composition and the volume fraction of the γ phase. Thus, a continuously changing Curie temperature was observed until the temperature reached 632°C.

The Curie transformation can be observed from the DSC heat flow curve, where a small but still distinguishable peak occurs at 632°C on cooling, in good agreement with the TG curve change.

For the presence of the peak at 760°C, if we analyze the DSC heat flow curve, we can propose a second hypothesis. Nishizawa[22] reported a horn-shaped two-phase region in Co containing ferromagnetic binary alloys, indicating the occurrence of ferromagnetic and paramagnetic phase separation. In the present case there might also be a Nishizawa horn

existing in the Al-Co-Ni system, as is predicted using the Thermo-Calc® TCNI8 database and shown in the isothermal section, Fig. 1. However, this phase separation has until now never been verified experimentally. Looking at the DSC curve, the peak at 760°C can be explained by a phase separation corresponding to a Nishizawa horn. The thermal effect is larger than one would expect for a second order transition and there is another heat effect at 632°C that corresponds to the main Curie temperature transition. Combined with the TG data, it shows that this process is reversible after the first heating cycle (Fig. 2b). The slow change in apparent mass might be due to the two-phase separation in the Nishizawa horn as the narrow two-phase region traverses this alloy composition as a function of temperature. The result would be that a small amount of ferromagnetic phase would form initially, the amount of which increases with decreasing temperature. Consider an alloy composition which is single-phase γ_p (paramagnetic γ phase), on decreasing the temperature the alloy composition enters the two-phase field $\gamma_p+\gamma_f$, resulting in the formation of γ_f (ferromagnetic γ phase) within the paramagnetic phase. This is a diffusion controlled process since the two phase compositions are different. This transformation will be indicated by an apparent mass increase depending on the amount of γ_f formed. As the temperature is lowered the phase fraction of γ_f increases and the composition of γ_f changes resulting in a changing Curie temperature until the two-phase field passes the alloy composition. Since this is a diffusion controlled, first order transformation there will be a hysteresis between heating and cooling, as is indeed experimentally observed. Once the narrow two-phase region has passed, the alloy once again becomes a single phase alloy consisting of γ_f on cooling and γ_p on heating. The microstructural observation of this transformation is difficult as for any given alloy composition the two-phase region occupies

a narrow temperature window. However, our magnetic balance technique offers indirect evidence for the existence of the Nishizawa horn. This demonstrates that the combined analysis of heat flow and thermogravimetry in a magnetic field can give us a clearer understanding of the phase transformation behavior during thermal cycling involving ferromagnetic phases.

For the second cycle, Fig. 2b), a similar result was observed with the difference from Cycle 1 being with the first heating. The heating and cooling TG curves are almost identical in the second cycle. Neither of the curves has a sharp Curie transformation, instead a slow apparent mass change was found between 634 and 760°C, similar to Cycle 1 cooling. This temperature range also corresponds to the Thermo-Calc® prediction for the Nishizawa horn covering the Ni 35-4 composition from 600 to 720°C. The slow apparent mass change during second heating indicates a possible dissolution of the precipitate phase, which might be due to the existence of the Nishizawa horn as discussed above. The initial state of the sample after quenching from 1100°C after homogenization for 24h, is single γ phase. As a result, the apparent mass change is sharp during the first heating.

We have also used a different heating rate (10°C/min) on alloy Ni 35-4 and compared that with 5°C/min, as shown in supplementary Fig. S1. The results indicate a hysteresis in the transformation, which suggests that it is a diffusional transformation. Supplementary Fig. S2 shows the TG-DSC curves of Ni 35-4 without applied magnetic field. It can be seen that the buoyancy effect (the mass change caused by protective gas flow and turbulence in the DSC during heating and cooling), causing a change of less than 1mg over 1200 degrees, is negligible compared with the magnetic transition effect.

From the above results, the Curie temperature of Ni 35-4 could be determined from

the second heating cycle as 720°C.

3.2 10 at.%Al

When the Al content is increased to 10 at.%, as shown in Fig. 3, the TG-DSC curves indicate a more complicated Curie transformation. The microstructure of Ni 40-10 at the beginning of the first heating cycle is single γ phase. The two cycles exhibit similar curves in shape. From both curves, the characteristic Curie transformation temperature during heating is about 40°C higher than that during cooling. This is likely because on heating the γ phase has a low Al content due to γ' precipitates being present, so the Curie temperature is higher. While on cooling, the precipitation starts around 781°C. Therefore, the Al content in γ phase is higher, hence the lower Curie temperature.

Steps are present on the TG curves on both cycles above 670°C. On cooling there is a slow increase in apparent mass on the TG curves indicating a gradual increase in the magnetic susceptibility or quantity of ferromagnetic phase starting from 783°C. As shown in supplementary Fig. S3, when annealing at 600°C, discontinuous precipitation of γ' is observed. Based on the previous discussion, one possible reason that could account for the presence of the step might be due to the precipitation of the γ' phase which depletes the composition of the Al in the γ matrix in that region. As a result of this, the γ matrix composition changes, increasing the fraction of ferromagnetic γ phase or magnetic susceptibility of the sample correspondingly. The heating curve is consistent with the reverse process. The two small peaks that appear on the DSC curves during both heating and cooling processes correspond to the Curie transformations. Based on this result we can establish the γ' solvus temperature for this alloy as 782°C, which agrees with the

experimental phase diagram results[9] as well as Thermo-Calc® predictions.

Ni70-10:

In Fig. 4, when the Co content increases to 70 at.%, the curves become simpler. The starting microstructure of Ni 70-10 is single γ phase after quenching from 1200°C. From the TG curves, it can be seen that there is little difference between the heating and cooling processes for both cycles. The Curie transformation is quite sharp at around 780°C without any steps compared with the previous Ni 40-10 sample, which suggests that this is a single-phase magnetic transformation. The effective mass change resulting from the ferromagnetic transformation is very reproducible in both cycles, indicating that the amount and composition of the ferromagnetic phase is reproduced.

Examining the DSC curves, two more peaks were found during heating and cooling for both cycles, at around 660°C and 590°C, respectively. The peaks indicate a dissolution and precipitation of second phase occurring below the Curie temperature, which is not reflected on the TG curves. The optical microstructures in Fig. 12 of our prior publication [9] confirm the occurrence of discontinuous precipitation at low temperature (600°C). Due to the high Co content, the Curie temperature is higher than the γ' solvus temperature which we determine from the DSC heating curve to be 664°C and in this case the precipitation phenomenon has no effect on the observed Curie temperature.

3.3 15 at.%Al

When Al content is increased to 15 at.%, Ni 10-15, Fig. 5, the two curves for both cycles show that the Curie transformation temperature is significantly lower, at a temperature of about 320°C, than for the lower aluminum content samples discussed

previously. This is expected as addition of Al to either Co or Ni produces a rapid decrease in Curie temperatures as can be seen from the binary phase diagrams[23]. There are small peaks on the DSC curves on cooling corresponding to the Curie temperature, which in the absence of the TG signal could be missed. For the TG curves, on Cycle 1, there is a large temperature difference between the Curie transformation on heating and cooling, with the transition on heating being 100°C lower than on cooling. This suggests that a composition change occurs for the ferromagnetic phase due to the cycling. At the end of the first cooling cycle, the apparent sample mass is 6 mg higher than at the beginning of the heating stage. This could be the result of either an increased magnetic susceptibility because of a compositional difference or a larger volume fraction of the ferromagnetic phase. For Cycle 2, the TG curves during the heating and cooling processes are quite similar, with the drop on heating occurring at a slightly higher temperature than on cooling.

The reason for the large Curie temperature difference between heating and cooling on Cycle 1 might be due to the precipitation of γ' phase out of the matrix since the nominal sample composition falls into a γ+γ' two-phase region below about 800°C. This would increase the Co composition of the γ phase after heating up to 880°C and cooling back down compared with the starting as-quenched composition. This also explains the mass change after the first cooling cycle resulting from an increase in magnetic susceptibility due to the phase composition change in the γ phase.

3.4 20 at.%Al

Fig. 6 shows the result for Ni 40-20, the sample containing 20 at.%Al. Only peaks corresponding to the Curie transformation temperatures can be found on the heat flow

curves during both cycles. The starting microstructure of Ni 40-20 consists of γ and β phases after quenching from the homogenization temperature. Examining the TG curves, for the first cycle, the curve was found to have a large magnetic force increase at the end of the cooling process compared with the value at the beginning of heating. The initial apparent mass is only 10mg, while after cooling the resulting apparent mass increased to 32mg. The increase in TG can be due to two possible reasons: an increase in the magnetic susceptibility if there is a change in the composition of the ferromagnetic phase; or an increased amount of ferromagnetic phase. While in this case the increase in TG should be due to an increase in the amount of the ferromagnetic phase. This is why we performed a second thermal cycle for verification of the reversibility of the samples' thermal behavior. For Cycle 2, it becomes easier to observe a very sharp Curie transformation between 670 and 700°C with a 30°C lag between the heating and cooling processes. It is also noticeable that the low temperature segment curve is not as flat as in the first three samples as discussed above with lower Al contents. From the phase diagram, the sample composition of Ni 40-20 falls into a γ+β two-phase region. Moreover, from supplementary Fig. S4, it could be seen that when aging at lower temperature (600°C), the decrease in solubility results in simultaneous precipitation in both γ and β phases. The precipitation of γ from β accounts for an increasing amount of the ferromagnetic phase and thus increases total apparent mass below the Curie temperature. Therefore, the TG behavior can be explained as the gradual precipitation and compositional change of the ferromagnetic γ phase that precipitates from the β matrix on lowering the temperature. In addition, the hysteresis in the Curie temperature curve is consistent with a diffusional process such as precipitation.

3.5 25 at.%Al

When the Al content is increased to 25at.%, Ni 25-25, the sample composition falls in the γ+β two-phase area at the homogenization temperature of 1100°C and enters a γ+β+γ' three-phase area at temperatures lower than 800°C[9]. The TG-DSC results are shown in Fig. 7. For the heating TG curves, there is a large difference between the two thermal cycles. For Cycle 1, an apparent mass increase occurs between the initial state corresponding to the sample quenched from 1100°C and the end of the cooling process, suggesting that additional magnetic phase precipitated from the matrix during the first heating and cooling cycle. There is an interesting phenomenon on the first heating curve between 560 and 650°C. The TG curve first decreases on heating to 564°C, then rises until 650°C and then drops to 0 mg at 700°C. The reason for the first decrease might be due to the relatively low Curie temperature of the ferromagnetic phase present after quenching since the sample composition has low Co content and high Al amount. As a result, at temperatures higher than 500°C, the Curie transformation started, decreasing the TG value. Meanwhile, combining the microstructure changes as described previously[9], as the temperature rises, additional γ' phase precipitates out, resulting in a Co content increase in the γ phase composition. From the TG curve, we could estimate the temperature at which a significant change in the γ phase composition takes place to be around 564°C.

During the second cycle, the curve becomes simpler with a higher Curie transformation temperature on heating than on cooling. The cooling segments in Cycle 1 and 2 are identical. Between RT (room temperature) and 650°C there is a gradual decrease in magnetic force on heating for Cycle 2 before the sharp drop at the Curie temperature. There is a notable exothermic peak on the heat flow curve on heating around 350°C which is only

present in Cycle 1. A small decrease on the TG curve corresponding to the effect at 350°C was also observed. This implies that there is an irreversible transformation occurring since it is not present on the second cycle. The larger drop in TG between 450 and 564°C is accompanied by a broad exothermic effect on the first heating cycle when compared with the second, consistent with a precipitation phenomenon. The small peaks above 1000°C on the DSC curves indicate a possible heat effect caused by the movement of the γ+β phase field boundaries at high temperatures.

3.6 30 at.%Al

Finally, for Al content of 30 at.%, Ni 50-30, the results are shown in Fig. 8. The starting microstructure of Ni 50-30 is single phase β. It can be seen from the TG curve that a similar trend was found as that in sample Ni 40-20, Fig. 6. The first heating process in Cycle 1 results in a decrease in the apparent mass at near room temperature, but not to zero, followed by gradual increase up to around 650°C, then a rapid increase and finally a decrease to zero. In Cycle 1, a significant apparent mass increase was observed after first cooling compared with the initial state of the sample. This indicates the appearance of newly precipitated magnetic γ phase since the two high-Al samples both fall into the γ+β two-phase region below 1100°C. The microstructures in Ref.[9] show that on cooling, due to a decrease in solubility, the needle-shape precipitation of γ from β phase starts to appear at 800°C and continues to grow at 550°C. In this sample some interesting phenomena occur on the DSC curves. Apart from the two peaks at 686°C and 704°C on Cycle 1 (similar position on Cycle 2), which indicate the Curie transformation temperature on the cooling and heating segments, additional small peaks were observed at higher temperatures on both

cycles. The peak at 1054°C on the first heating cycle is likely due to the dissolution of γ phase. During cooling, the peak appearing at 1027°C indicates the precipitation of the γ phase.

4.Discussion

4.1 Curie temperature summary

From the results above, the Curie temperature and thermal behavior of the samples were investigated after two cycles of heating and cooling. As can be seen, for some of the samples, there are significant differences on the TG curves between Cycle 1 and Cycle 2 due to the initial super-saturation of samples in an as-quenched state. Therefore, it is reasonable to determine the Curie temperatures from the heating and cooling curves on Cycle 2.

All of the original TG data were obtained and analyzed in a wavelet analysis method using Python code[21]. The Curie temperature was automatically found as the temperature where the apparent sample mass reached zero during the second heating and cooling process. These data were compared with data obtained from standard magnetic reference samples including pure Ni, pure Fe, pure Co and Alumel with the same testing conditions and mean and standard deviations were calculated for the Curie temperature. The final analyzed results are shown in Table 2. In previously published work.[24], for alloy Co37Ni35Al28 annealed at 1373K, a Tc of 1055K was found for the γ phase. Among the samples investigated in our work, the sample with closest composition is Ni30Co40Al30, with a Tc of 741°C (1014K), which is slightly lower than that in the prior work. The difference lies in two aspects: 1) the different amount of γ phase in these two slightly

different compositions; 2) the higher Co amount and lower Al amount, making the Tc slightly higher than that in Ni30Co40Al30. The result in the current work therefore agrees well with the prior data.

Multiple phases might exist in the alloys but the measured Curie temperatures correspond only to the ferromagnetic γ phase. As a result, a ternary Curie temperature contour plot for the γ phase was constructed, as shown in Fig. 9. The graphs show the Curie temperature change as a function of the γ phase composition. The Curie temperature of pure Co is 1124°C and that of pure Ni is 349°C. Therefore, a general descending trend of the Curie temperature can be observed, starting from the high-Co, low-Al end gradually down to the low-Co, high-Al end. It can also be seen that there is a plateau appearing at the high to mid Co content region. The measured Curie temperature plot agrees well with the Al-Co-Ni phase diagram, suggesting that samples with high Co, low Al content exhibit higher Curie temperatures due to the location of the single γ phase area. As Co content decreases and Al increases, the sample compositions fall into the β+γ two-phase region, resulting in a gradual change of the Curie temperature and with decreasing Co, the appearance of γ' phase leads to a sharp drop in the Curie temperature.

The temperature contour map provides a tool for predicting the Curie temperature in the Al-Co-Ni system. From the plot, a nonlinear surface fitting was made using the Exponential2D model[25] using a Levenberg-Marquardt iteration algorithm[26]. The fitted result for the Curie temperature *z*, in Kelvin, is shown below:

$$z = 1385 - 1273*\exp(-x/178)*\exp(-y/46) \quad (1)$$

Where *x* and *y* are the Ni and Co compositions in atomic %, respectively. The constants are generated from the fitting results. From this it is possible to predict the estimated Curie

temperatures in the γ phase in the Al-Co-Ni system at a given alloy composition. We estimate the error between the fit and measured Curie temperatures to be within 3%. For example, for a given alloy Ni 40-20, x=40, y=40; from the above equation, z is calculated to be 959K(686°C), close to the experimental value in Table 2, 992K (719±12°C).

In order to investigate the TG behavior as a function of phase fractions and alloy compositions, the mass (TG) increase effect is also summarized and listed in Table 2. This is calculated by comparing the apparent mass increase in the applied magnetic field with the initial sample mass without applied magnetic field. A ternary contour plot was obtained, and is shown in supplementary Fig. S5, superimposed on the previously published Al-Co-Ni 1100°C isothermal section[9] for comparison. The TG effect varies in different phase regions due to the difference in phase fraction and magnetic susceptibility of the phases. There are three maxima of the mass increase observed at: Ni-50Co, Ni 22-20 and Ni 50-30. There is no simple model to predict the apparent mass change since it depends on the fraction and composition of the ferromagnetic phase both of which change with temperature and indeed, with heating and cooling rates when diffusional transformations occur. The change in TG effect qualitatively reflects the differences in phase fractions and alloy compositions, which are the two major factors affecting the apparent mass change in the magnetic field. Near Ni-50Co, the sample has a higher magnetic field induced mass increase as the sample contains no Al. For samples near Ni 22-20, the TG increase reaches a local maximum due to a higher amount of Co element and γ phase; also no β phase exists in this region. In the Ni 50-30 region, although the sample contains a higher content of Co, the sample is located in the γ+β two-phase region; the existence of β phase prevents the TG from increasing further. It should be noted that all the TG increase effects were calculated

using the mass change from the second thermal cycle in order to ensure good data repeatability. The superimposed isothermal section is only a guide for locating the phase regions. Despite this limitation, the observed TG behavior is in good agreement with the phase diagram and the ternary contour map can provide a good estimation of the TG increase effect in the Al-Co-Ni alloy system.

4.2 Existence of the Nishizawa horn

Although the existence of a Nishizawa horn in the Al-Co-Ni system has been predicted using Thermo-Calc® with the TCNI8 database, no experimental observations have been reported. Fig. 10 shows two calculated vertical sections of Al-Co-Ni alloy system with 4 at.% and 10 at.% Al, respectively, computed using Thermo-Calc®, and the phase areas are labeled correspondingly. The estimated secondary magnetic ordering (Curie) temperature line based on the fitting model in Section *4.1* and the position of the Nishizawa horn is indicated on Fig. 10 a). The Curie temperature after phase separation is given by the two, three or four phase boundaries that include the γ_f phase. The vertical section gives a more straightforward description of the phase transformations in Al-Co-Ni alloys as a function of temperature. At 4 at.% Al content, the miscibility gap between γ_p and γ_f forms a *horn* shape with increasing Co content. The 800°C boundary compositions can be located on the calculated isothermal section for additional perspective, in particular the orientation of tie lines which are not in the plane of the vertical section. Moreover, no other phases exist above the γ_p phase boundary. As a result, the Nishizawa horn can be observed directly from the isothermal section at 800°C. While at 10 at.% Al, there is a four-phase invariant reaction $\beta+\gamma_p \rightarrow \gamma'+\gamma_f$ that occurs just above 800°C, illustrating the phase transitions

including the Nishizawa horn, as has been described elsewhere[9]. Therefore, the γ_p and γ_f two-phase region at 800°C is extremely small and hence can not be seen on the isothermal section.

Although the vertical sections indicate the phases present at any temperature they do not indicate the phase compositions since tie lines may not be in the plane of the vertical section. Nevertheless we can use such a section to help understand the behavior of an alloy during the thermal cycling in the magnetic TG-DSC experiment. The alloy Ni 40-10 shows a main Curie temperature effect at about 675°C and then a gradual decrease in the TG signal to zero at 781°C. The vertical section indicates that on heating the decrease in amount of ferromagnetic phase begins at 649°C and then is completed at 699°C. Although the upper temperature is in poor agreement with the experiment the overall behavior is consistent with a gradual change in the ferromagnetic phase amount as indicated by increasing the temperature through the three-phase region on the vertical section. The Ni 70-10 alloy has a single Curie temperature around 740°C and this is consistent with the prediction of the vertical section that on heating or cooling the alloy goes through the four-phase reaction at about 800°C so that the transformation from ferromagnetic to paramagnetic occurs at a single temperature or a very narrow temperature range. From our experiments the transformation is close to 800°C indicating good agreement with the Thermo-Calc® prediction.

In addition to the results for the Ni 40-10 alloy, the gradual change in the TG curve in a magnetic field for Ni 35-4 can also be interpreted as due to the existence of a two-phase, ferromagnetic-paramagnetic region, i.e. the Nishizawa horn. In order to verify this assumption, we synthesized two additional alloy samples, Ni 45-4 and Ni 25-4. The

compositions were chosen according to our calculated Thermo-Calc® results, where the horn goes from the high-Co end with decreasing temperature from 800 to 600°C. The Curie transformation temperature (or temperature range of the gradual change in the TG curve) should decrease from Ni 45-4 to Ni 25-4. Fig. 11 shows the TG and DSC curves of Ni 45-4 and Ni 25-4, which are very similar to Ni 35-4. In Fig. 11, for Ni 45-4, there is a slow apparent mass change observed between 728 to 818°C (Cycle 2); while this temperature range decreased to 655~730°C for Ni 35-4 (Cycle 2) (Fig. 2) and further down to 558~643°C (Cycle 2) for Ni 25-4. These results agree well with our original assumption that the slow change in TG curve is due to the existence of the Nishizawa horn, which leads to a ferromagnetic and paramagnetic two-phase separation in the γ phase. Since the transformation is diffusion controlled one would expect that there will be some hysteresis between heating and cooling and this is observed for all 3 alloys. The hysteresis effect is also observed when the scan rate is changed as shown in supplementary Fig. S1. This is the first time that experimental evidence has been presented indicating the existence of a Nishizawa horn in the Al-Co-Ni system supporting the prediction using Thermo-Calc® [9,22].

5. Summary and Conclusions

The Curie temperature in the Al-Co-Ni alloy system was measured using a combined magnetic TG and DSC method. This method provides a powerful technique for detecting phase transformations and precipitation through thermo-magnetically analyzing the behavior of alloys in which at least one phase is ferromagnetic. We generated a nonlinear surface fitting function of the measured Curie temperatures based on the Exponential2D

model. The function is helpful for the prediction of Curie temperature of the γ phase in the Al-Co-Ni alloy system. The following conclusions can be made:

1) From the contour map, the Curie temperature decreases from high Co, low Al compositions to low Co, high Al compositions passing through a sloping plateau at mid Co content.

2) The present results provide the first experimental evidence for the occurrence of a Nishizawa horn in the Al-Co-Ni system as predicted using Thermo-Calc®.

Acknowledgement

This work supported under National Science Foundation grant DMR 1607943 and by the Thermal Processing Technology Center at IIT. One of the authors, Yang Zhou is grateful for the financial support from the Chinese Scholarship Council. The authors wish to thank Dr. Ricardo Schwarz for a critical review of the manuscript and Weiwei Zhang of Thermo-Calc Software Inc. for assistance with the Thermo-Calc computations.

Author Contributions

Philip Nash conceived the idea and Yang Zhou performed the experimental work at Illinois Institute of Technology. Both authors contributed equally to the analysis of the experimental data. The manuscript was written through contributions of all authors and reviewed by all authors.

Declaration of interest: None.

References

[1] K. Oikawa, T. Ota, F. Gejima, T. Ohmori, R. Kainuma, K. Ishida, Phase Equilibria and Phase Transformations in New B2-type Ferromagnetic Shape Memory Alloys of Co-Ni-Ga and Co-Ni-Al Systems, Mater. Trans. 42 (2001) 2472–2475.

[2] K. Oikawa, L. Wulff, T. Iijima, F. Gejima, T. Ohmori, A. Fujita, K. Fukamichi, R. Kainuma, K. Ishida, Promising ferromagnetic Ni–Co–Al shape memory alloy system, Appl. Phys. Lett. 79 (2001) 3290–3292.

[3] Z. Liu, S. Yu, H. Yang, G. Wu, Y. Liu, Phase separation and magnetic properties of Co–Ni–Al ferromagnetic shape memory alloys, Intermetallics. 16 (2008) 447–452.

[4] Y. Tanaka, K. Oikawa, Y. Sutou, T. Omori, R. Kainuma, K. Ishida, Martensitic transition and superelasticity of Co–Ni–Al ferromagnetic shape memory alloys with β+γ two-phase structure, Mater. Sci. Eng. A. 438–440 (2006) 1054–1060.

[5] Y. Tanaka, T. Ohmori, K. Oikawa, R. Kainuma, K. Ishida, Ferromagnetic Co-Ni-Al shape memory alloys with β+γ two-phase structure, Mater. Trans. 45 (2004) 427–430.

[6] W. Maziarz, Structure changes of Co–Ni–Al ferromagnetic shape memory alloys after vacuum annealing and hot rolling, J. Alloys Compd. 448 (2008) 223–226.

[7] R. Kainuma, M. Ise, C.-C. Jia, H. Ohtani, K. Ishida, Phase equilibria and microstructural control in the Ni-Co-Al system, Intermetallics. 4 (1996) S151–S158.

[8] Y. Zhou, P. Nash, T. Liu, N. Zhao, S. Zhu, The Large Scale Synthesis of Aligned Plate Nanostructures, Sci. Rep. 6 (2016) 1–8.

[9] Y. Zhou, P. Nash, S.M. Bessa, G.T. Ferrigatto, B.S.V.P. Madureira, A.S. Magalhães, A.

Oliveira, G.C. Pereira, L.G. Ribeiro, L.P. dos Santos, A.A. da Silva, J.D. Silva, A.G. Silva, J.M. de Souza, Y.S. Torres, R.L. da Silva, B.F.R.F. de Cunha, Phase Equilibria in the Al-Co-Ni Alloy System, J. Phase Equilibria Diffus. 38 (2017) 630–645.

[10] S. Chatterjee, M. Thakur, S. Giri, S. Majumdar, A.K. Deb, S.K. De, Transport, magnetic and structural investigations of Co–Ni–Al shape memory alloy, J. Alloys Compd. 456 (2008) 96–100.

[11] P. Villars, A. Prince, H. Okamoto, Al-Co-Ni, Handb. Ternary Alloy Phase Diagr. ASM Int. Mater. Park OH. 3 (1995) 3052–3063.

[12] M. Hubert-Protopopescu, H. Hubert, Aluminum-Cobalt-Nickel, VCH Verlagsgesellschaft, Weinheim, Germany, 1991.

[13] J. Schramm, The Nickel-Cobalt-Aluminum Ternary System, Z Met. 33 (1941) 403–412.

[14] V. Raghavan, Al-Co-Ni (Aluminum-Cobalt-Nickel), J. Phase Equilibria Diffus. 27 (2006) 372–380.

[15] X.L. Liu, G. Lindwall, T. Gheno, Z.-K. Liu, Thermodynamic modeling of Al–Co–Cr, Al–Co–Ni, Co–Cr–Ni ternary systems towards a description for Al–Co–Cr–Ni, Calphad. 52 (2016) 125–142.

[16] K. Enami, S. Nenno, Memory effect in Ni-36.8 At. Pct Al martensite, Metall. Trans. 2 (1971) 1487.

[17] C. Wang, A.A. Levin, L. Nasi, S. Fabbrici, J. Qian, C.E.V. Barbosa, S. Ouardi, J. Karel, F. Albertini, H. Borrmann, G.H. Fecher, C. Felser, Chemical Synthesis and Characterization of γ-Co2NiGa Nanoparticles with a Very High Curie Temperature, Chem. Mater. 27 (2015)

6994–7002.

[18]T. Saito, Magnetic properties of Co–Al–Ni melt-spun ribbon, J. Appl. Phys. 100 (2006) 53916.

[19]H. Seiner, J. Kopeček, P. Sedlák, L. Bodnárová, M. Landa, P. Sedmák, O. Heczko, Microstructure, martensitic transformation and anomalies in c′-softening in Co–Ni–Al ferromagnetic shape memory alloys, Acta Mater. 61 (2013) 5869–5876.

[20]S. Chatterjee, S. Giri, S. Majumdar, S.K. De, Compositional variation of magnetic properties in Ni71−xCoxAl29 alloys, J. Alloys Compd. 477 (2009) 27–31.

[21]J. Hasier, M.A. Riolo, P. Nash, Curie temperature determination via thermogravimetric and continuous wavelet transformation analysis, EPJ Tech. Instrum. 4 (2017) 5.

[22]T. Nishizawa, M. Hasebe, M. Ko, Thermodynamic analysis of solubility and miscibility gap in ferromagnetic alpha iron alloys, Acta Metall. 27 (1979) 817–828.

[23]F. Stein, C. He, N. Dupin, Melting behaviour and homogeneity range of B2 CoAl and updated thermodynamic description of the Al–Co system, Intermetallics. 39 (2013) 58–68.

[24]B. Rajini Kanth, N.V. Ramarao, A.K. Panda, R. Gopalan, A. Mitra, P.K. Mukhopadhyay, Effect of annealing on the martensitic transformation of a CoNiAl ferromagnetic shape memory alloy, J. Alloys Compd. 491 (2010) 22–25.

[25]F. Brezzi, L.D. Marini, P. Pietra, Two-dimensional exponential fitting and applications to drift-diffusion models, SIAM J. Numer. Anal. 26 (1989) 1342–1355.

[26]J.J. Moré, The Levenberg-Marquardt algorithm: implementation and theory, in: Numer. Anal., Springer, 1978: pp. 105–116.

[27]T. Nishizawa, K. Ishida, The Co− Ni (Cobalt-Nickel) system, Bull. Alloy Phase Diagr. 4 (1983) 390–395.

Figure captions

Figure 1. Calculated isothermal section of Al-Co-Ni at 800°C (Thermo-Calc®, TCNI8 database, see text for explanation of legend).

Figure 2. The TG-DSC vs. Temperature curve for Ni 35-4: a) Cycle1 and b) Cycle2.

Figure 3. The TG-DSC vs. Temperature curves for Ni 40-10: a) Cycle1 and b) Cycle2.

Figure 4. The TG-DSC vs. Temperature curve for Ni 70-10: a) Cycle1 and b) Cycle2.

Figure 5. The TG-DSC vs. Temperature curves for Ni 10-15: a) Cycle1 and b) Cycle2.

Figure 6. The TG-DSC vs. Temperature curves for Ni 40-20: a) Cycle1 and b) Cycle2.

Figure 7. The TG-DSC vs. Temperature curves for Ni 25-25: a) Cycle1 and b) Cycle2.

Figure 8. The TG-DSC vs. Temperature curves for Ni 50-30: a) Cycle1 and b) Cycle2.

Figure 9. The Curie temperature contour. a) 3-D ternary Curie temperature graph; b) ternary contour projection.

Figure 10. Calculated vertical sections of Al-Co-Ni alloys with a) 4 at.% Al and b) 10 at.% Al using Thermo-Calc®.

Figure 11. The TG-DSC vs. Temperature curves for a) Ni 45-4 and b) Ni 25-4.

Tables

Table 1. Nominal composition and initial mass of Al-Co-Ni samples*

	Alloy ID.	Nominal Composition at.%			Sample Mass (mg)
		Ni	Co	Al	
1	Ni61Co35Al4	61	35	4	186
2	Ni50Co40Al10	50	40	10	272
3	Ni40Co50Al10	40	50	10	173
4	Ni30Co60Al10	30	60	10	183
5	Ni20Co70Al10	20	70	10	190
6	Ni39Co49Al12	39	49	12	150
7	Ni75Co10Al15	75	10	15	124
8	Ni58Co22Al20	58	22	20	128
9	Ni50Co30Al20	50	30	20	180
10	Ni40Co40Al20	40	40	20	172
11	Ni30Co50Al20	30	50	20	218
12	Ni20Co60Al20	20	60	20	167
13	Ni65Co10Al25	65	10	25	166
14	Ni50Co25Al25	50	25	25	135
15	Ni5Co70Al25	5	70	25	174
16	Ni50Co20Al30	50	20	30	135
17	Ni40Co30Al30	40	30	30	81
18	Ni30Co40Al30	30	40	30	129
19	Ni20Co50Al30	20	50	30	188

**Alloys 1 through 14 were ductile and could be cold rolled. Alloys 15 through 19 were too brittle for cold rolling.*

Table 2. Curie temperatures and standard deviations of the samples

Sample Material	Analyzed Curie Temperature (°C)	Standard Deviation (°C)	Sample Mass (mg) [a]	Apparent Mass increase (mg)	Mass increase effect [b]
Ni61Co35Al4	714	8	186	28	15.05%
Ni50Co40Al10	694	15	272	43.5	15.99%
Ni40Co50Al10	721	16	173	23	13.29%
Ni30Co60Al10	739	5	183	28	15.30%
Ni20Co70Al10	799	0	190	26	13.68%
Ni39Co49Al12	755	14	150	28	18.67%
Ni75Co10Al15	333	1	124	30	24.19%
Ni58Co22Al20	694	11	128	35	27.34%
Ni50Co30Al20	716	13	180	41	22.78%
Ni40Co40Al20	719	12	172	32.5	18.90%
Ni30Co50Al20	724	13	218	29	13.30%
Ni20Co60Al20	718	2	167	21.3	12.75%
Ni50Co25Al25	722	14	135	18	13.33%
Ni5Co70Al25	792	41	174	36	20.69%
Ni40Co30Al30	695	13	81	7.8	9.63%
Ni30Co40Al30	741	11	129	9	6.98%
Ni20Co50Al30	729	14	188	45	23.94%
Ni50Co50	873	1	173	40	23.12%
Pure Co	1124*	--	-	-	-
Pure Ni	349*	--	-	-	-

*: data from literature [27]

a) No magnetic field

b) Magnetic field applied

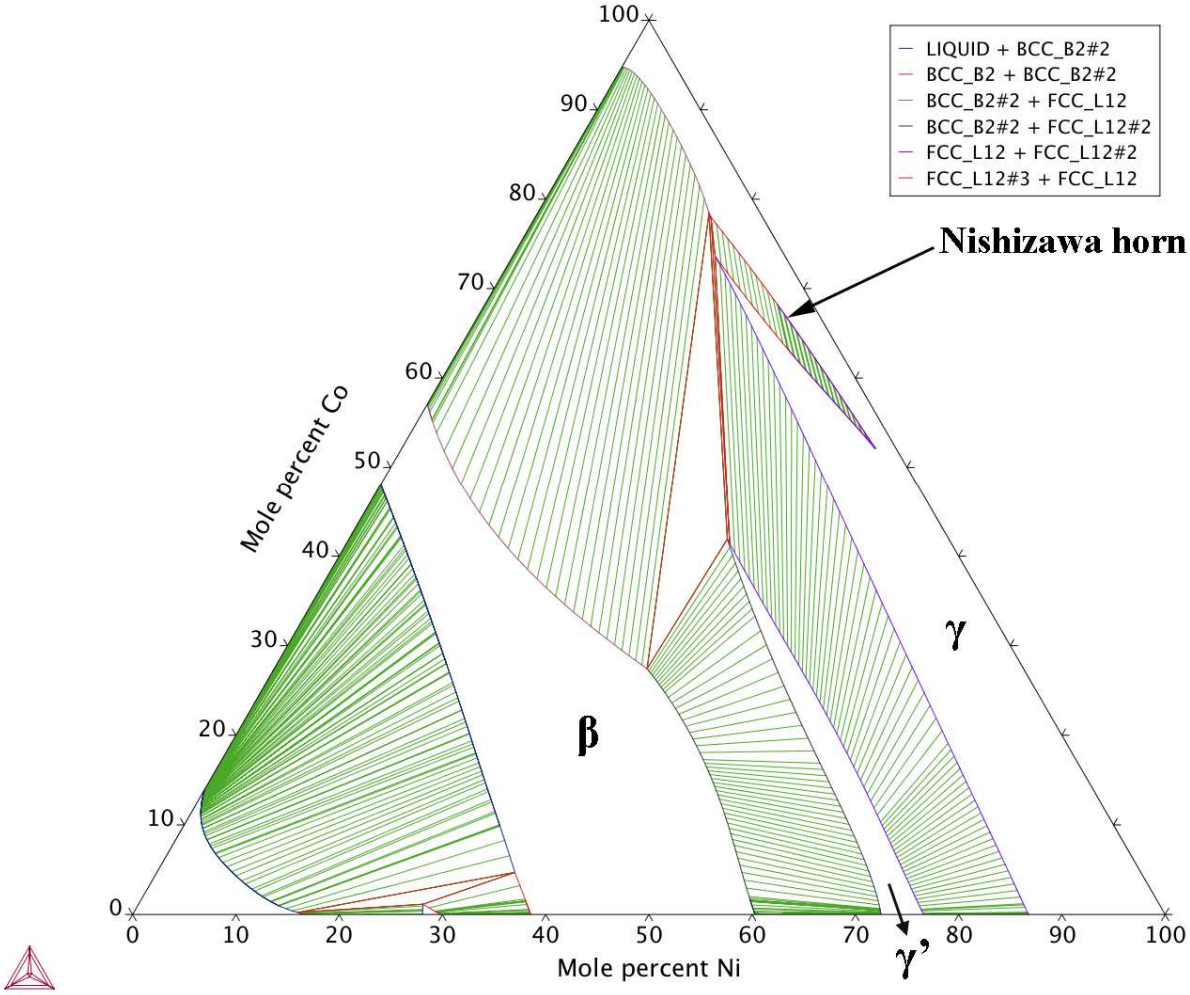
LIQUID + BCC_B2#2
BCC_B2 + BCC_B2#2
BCC_B2#2 + FCC_L12
BCC_B2#2 + FCC_L12#2
FCC_L12 + FCC_L12#2
FCC_L12#3 + FCC_L12
Nishizawa horn
β
γ
γ'
Mole percent Co
Mole percent Ni
0
10
20
30
40
50
60
70
80
90
100

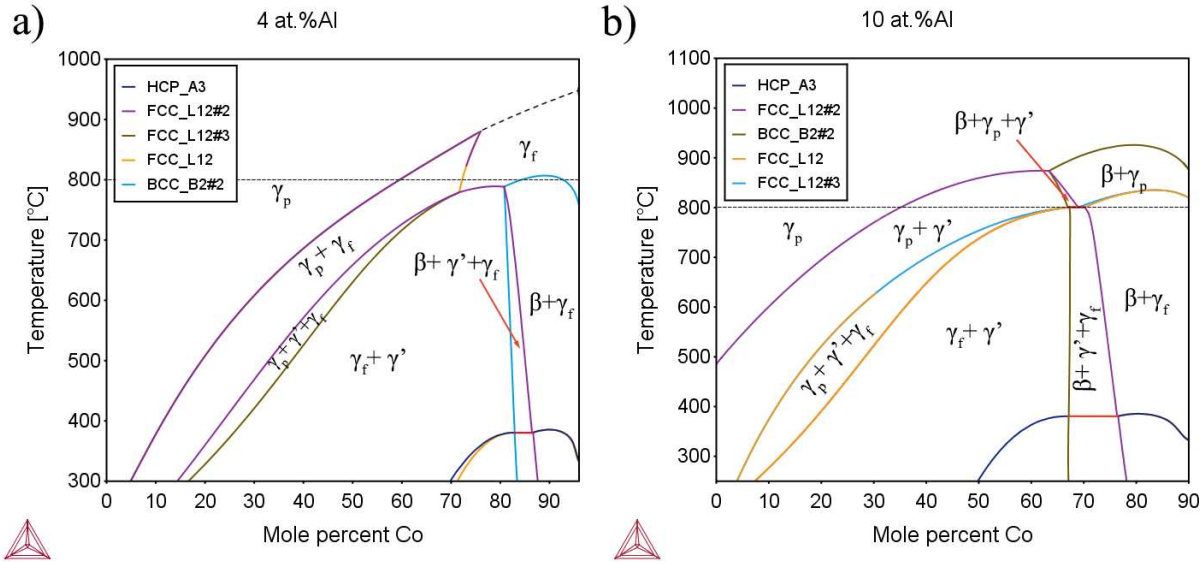

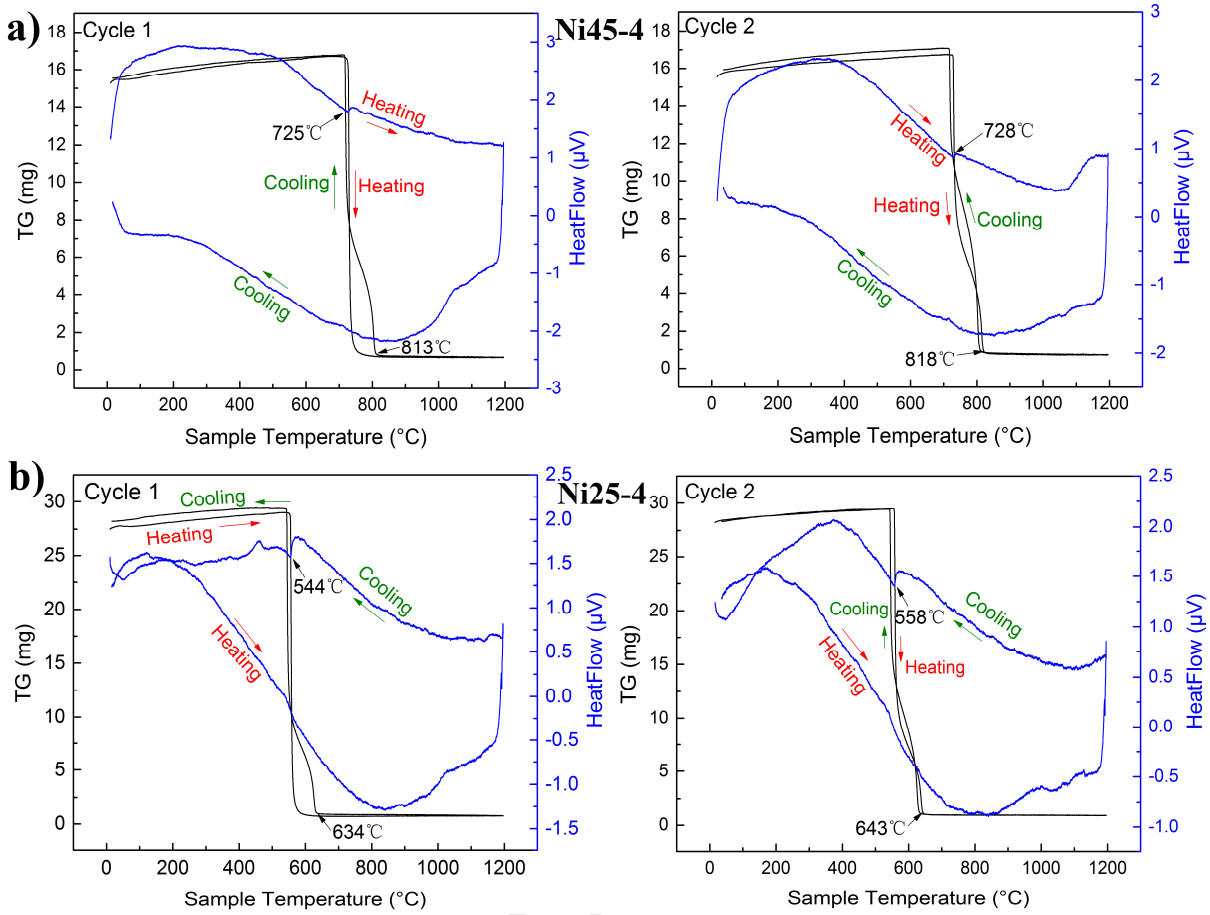
a)
Ni45-4
Cycle 1
Cycle 2
Heating
Cooling
725℃
813℃
728℃
818℃
TG (mg)
HeatFlow (μV)
Sample Temperature (°C)
b)
Ni25-4
544℃
634℃
558℃
643℃

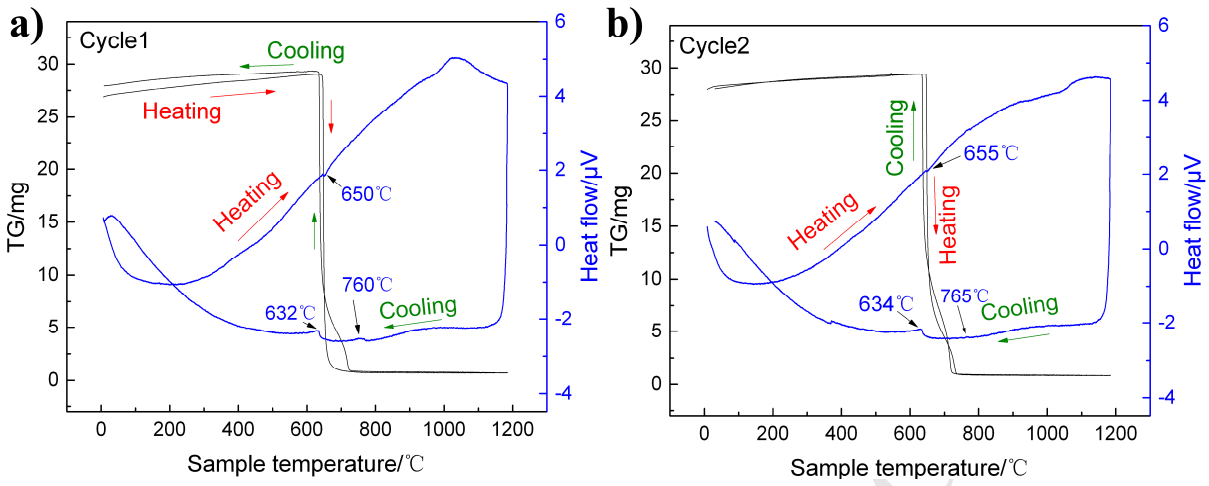

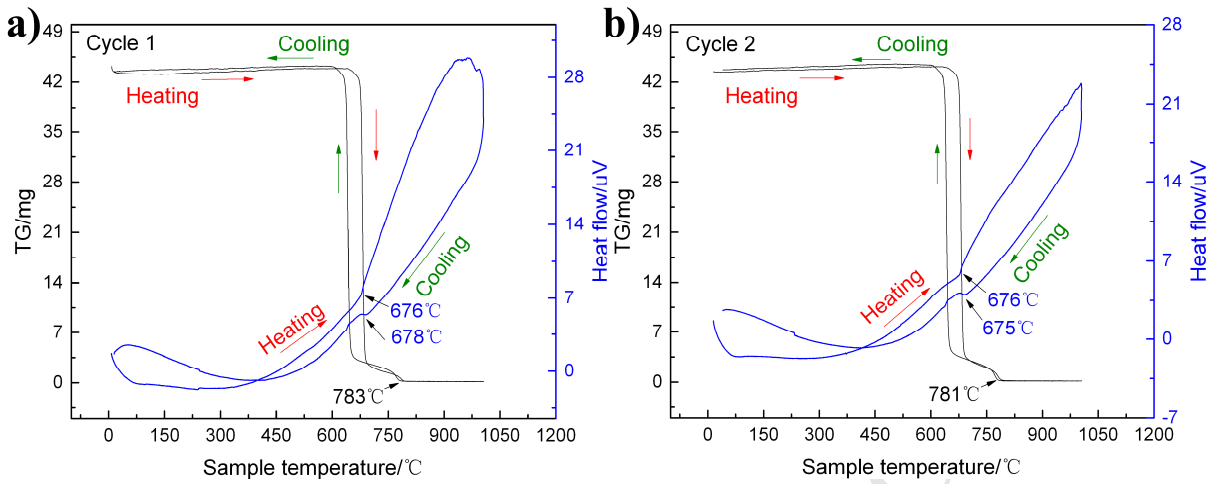

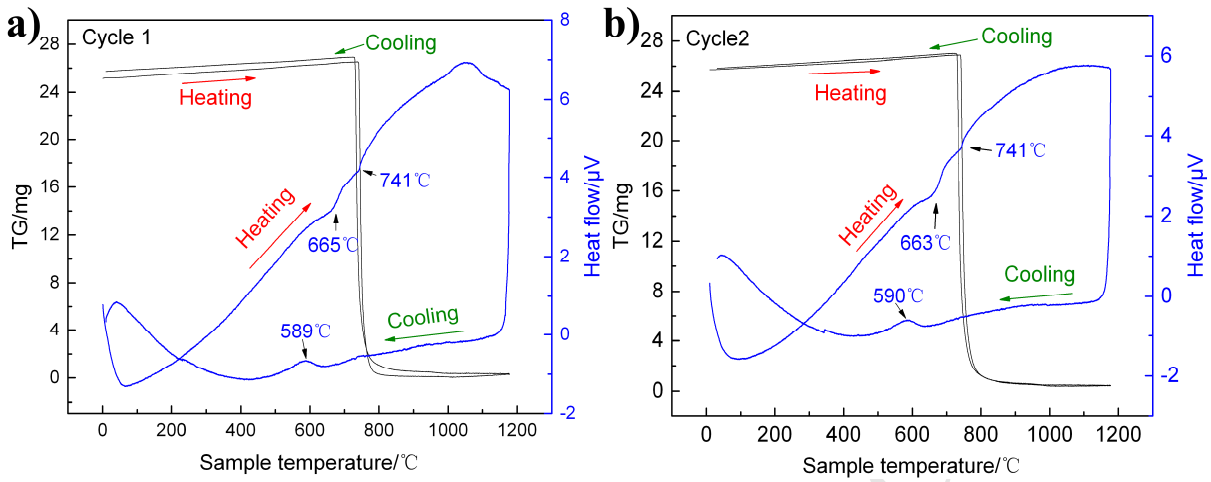

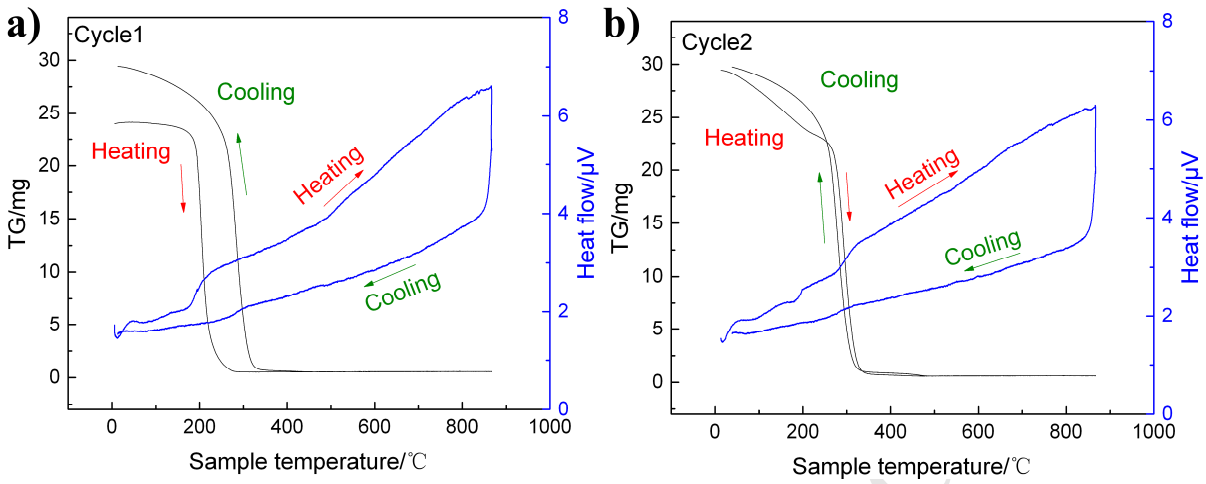

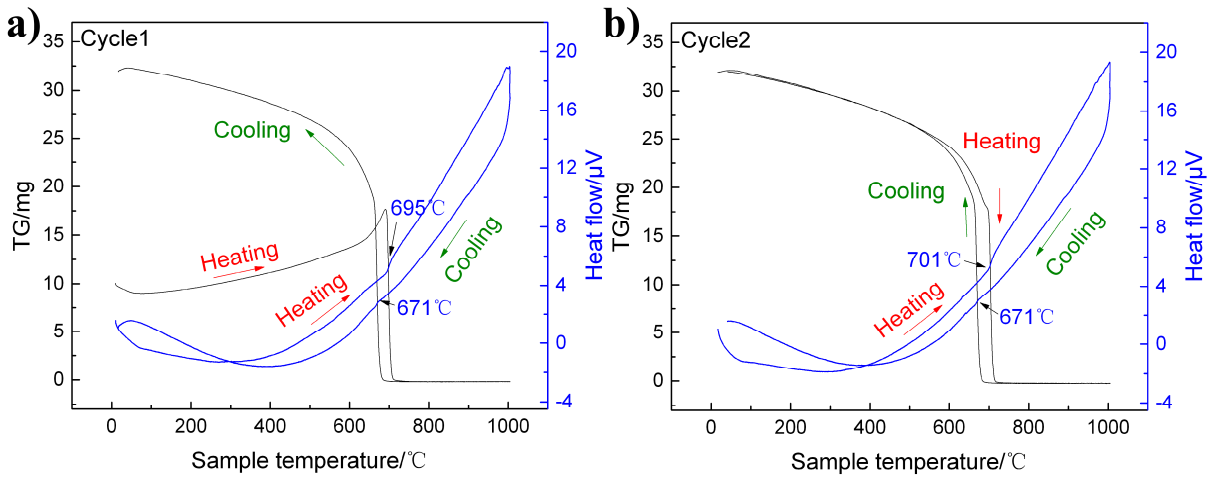

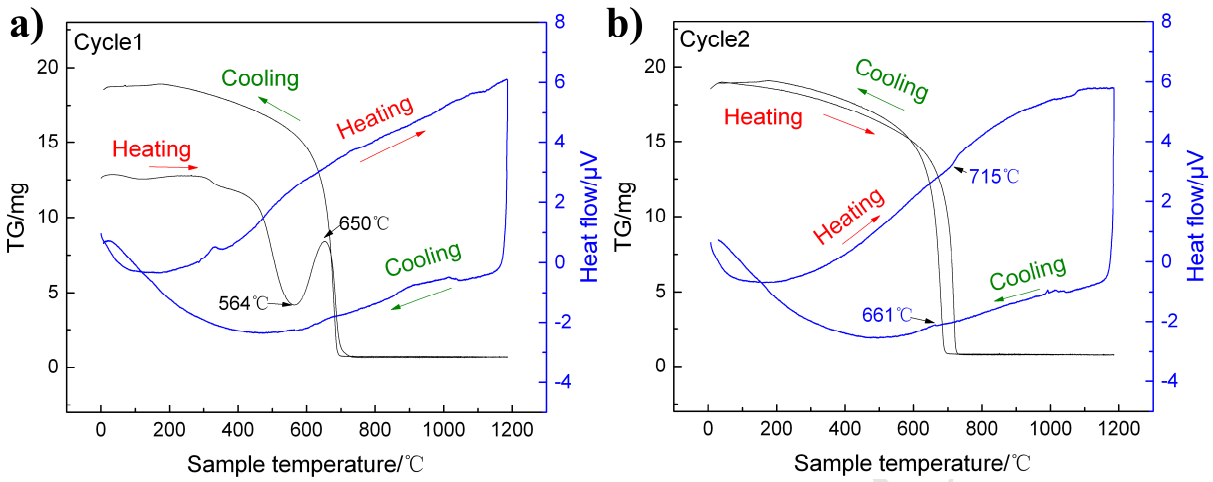

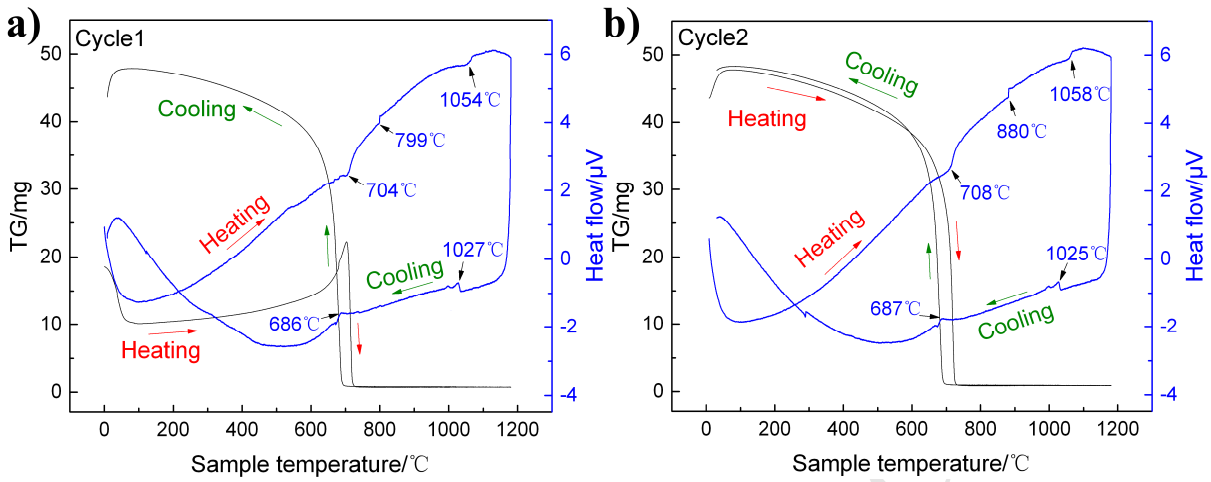

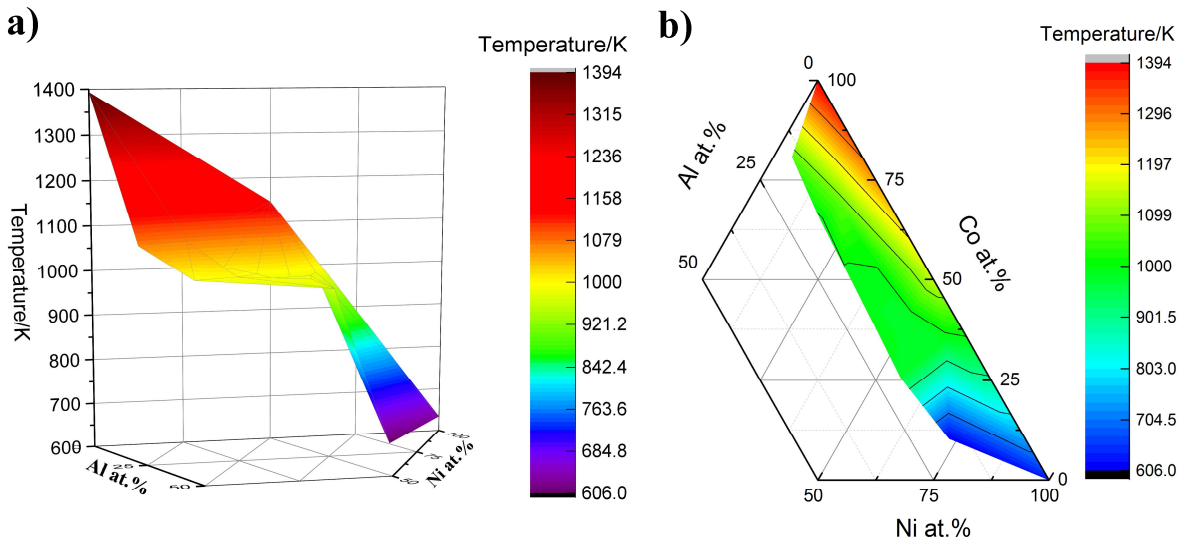

Highlights

- The Curie temperature in Al-Co-Ni system was measured using combined TG-DSC method
- A fitting function was proposed for estimating Curie temperature in Al-Co-Ni alloys
- This technique provides a novel method of detecting phase transformations
- Experimental results provide the first evidence for Nishizawa horn in this system